

Supplementary Information

„Chitosan supraparticles with fluorescent silica nanoparticle shells and nanodiamond-loaded cores”

T. Bollhorst, S. Jakob, J. Köser, M. Maas, and K. Rezwan

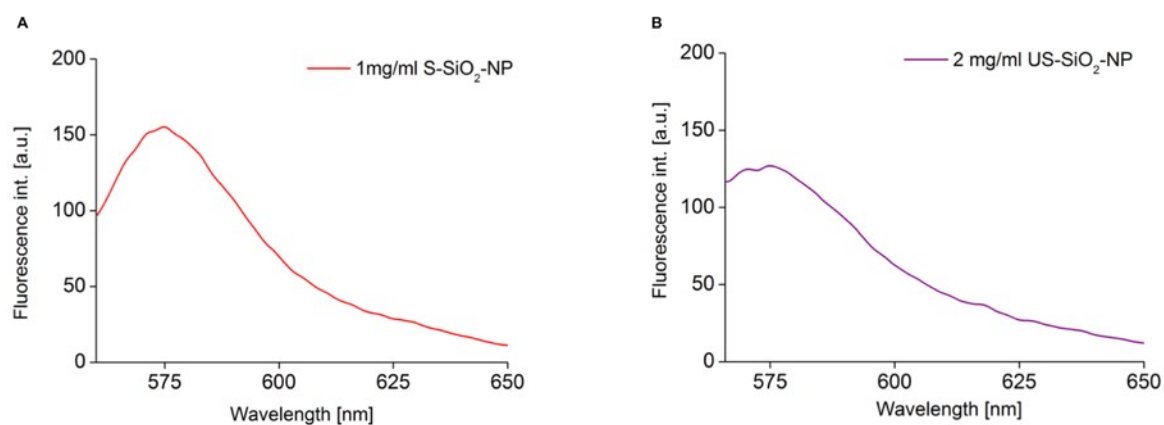


Fig. S 1: Fluorescence spectra of native A) S-SiO₂-NP and B) US-SiO₂-NP. For the dispersion of US-SiO₂-NP we were only able to detect a significant fluorescence intensity for higher (≥ 2 mg/ml) concentrations of particles.

Cell culturing, staining and imaging

Human osteoblasts cells (HOB) used in the experiments were cultured using protocols described in [1] and [2].

HOBs were seeded at a density of 3×10^4 cells in 800 μ l medium onto 15 mm Thermanox coverslips placed in 24 well polystyrene dishes at 37°C with 10% CO₂ and 95% relative humidity (RH) for 24 h. Fresh dispersions of NPs were prepared in phosphate buffered saline (PBS). After 24 h, the cells were exposed to 1 ml of PBS containing 100 μ g S-SiO₂-NPs for 2 h. Additional HOB samples with the absence of NPs were prepared as controls. After the exposure time, the cells were washed twice with PBS, to remove excess NPs and were subsequently characterized via fluorescent microscopic analysis. Fluorescent staining of the human osteoblast cells was performed using Alexa fluor 488 Phalloidin (AF488) for cytoskeleton and 4,6-diamidino-2-phenylindol (DAPI) for the cell nuclei. S-SiO₂-NPs were tagged with RBITC during their synthesis process. Cells were visualized using a fluorescence microscope (AX-10, Zeiss, Germany). Fig. S 2 shows HOBs unexposed (Fig. S 2-A) and exposed to S-SiO₂-NP (Fig. S 2-B.1 & -B.2).

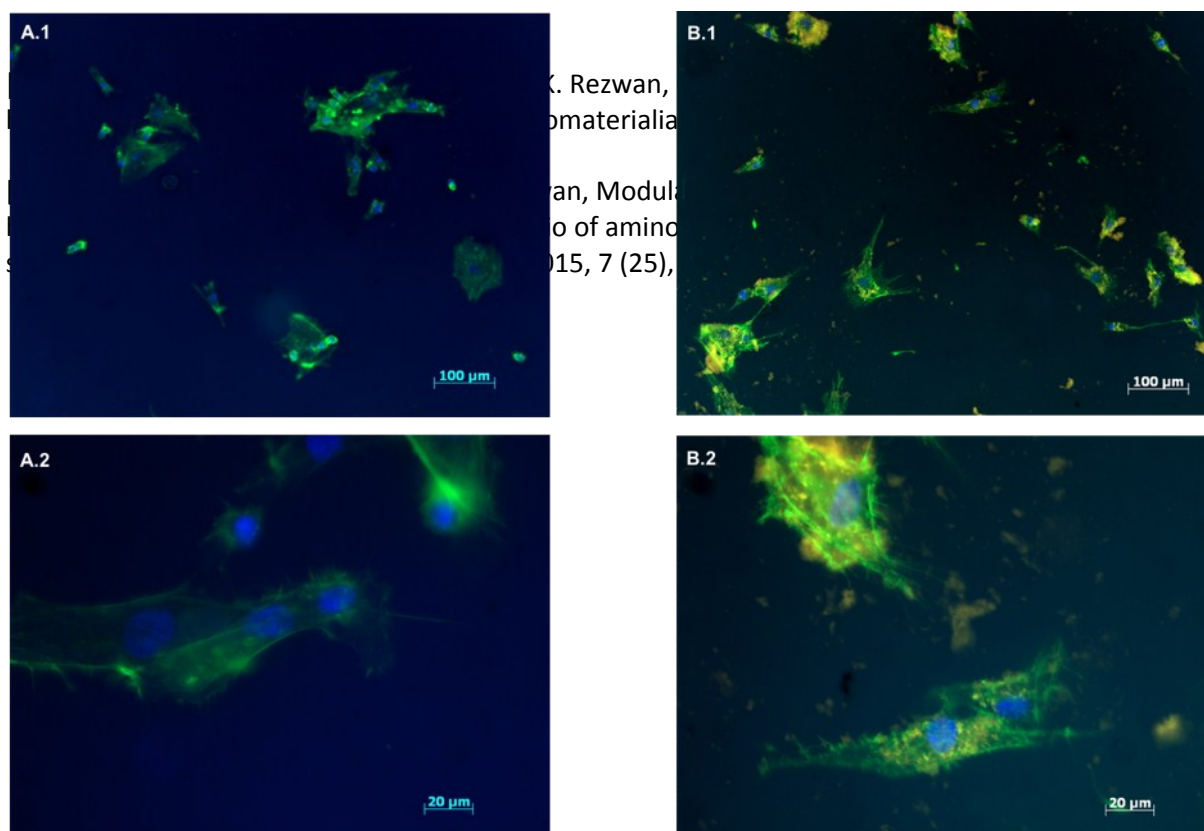


Fig. S 2: Fluorescence images of osteoblasts unexposed (A) and exposed to S-SiO₂-NP (B.1 and B.2). The particles can be identified in the inside and around the cells. Particles were not conjugated with any ligands and showed no specific intracellular accumulation in organelles. (blue: DAPI-nucleus, green: AF488-cytoskeleton, yellow: rhodamine labelled SiO₂ nanoparticles)

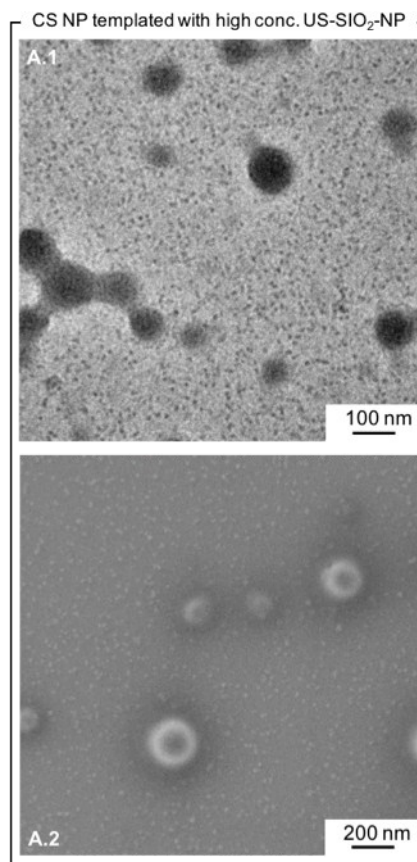


Fig. S 3: Templating attempt to synthesize chitosan particles with a high surface coverage of US-SiO₂-NP. As can be seen from the TEM and SEM micrographs, the increase of US-SiO₂-NP unfortunately led to a significant increase in free US-SiO₂-NP.

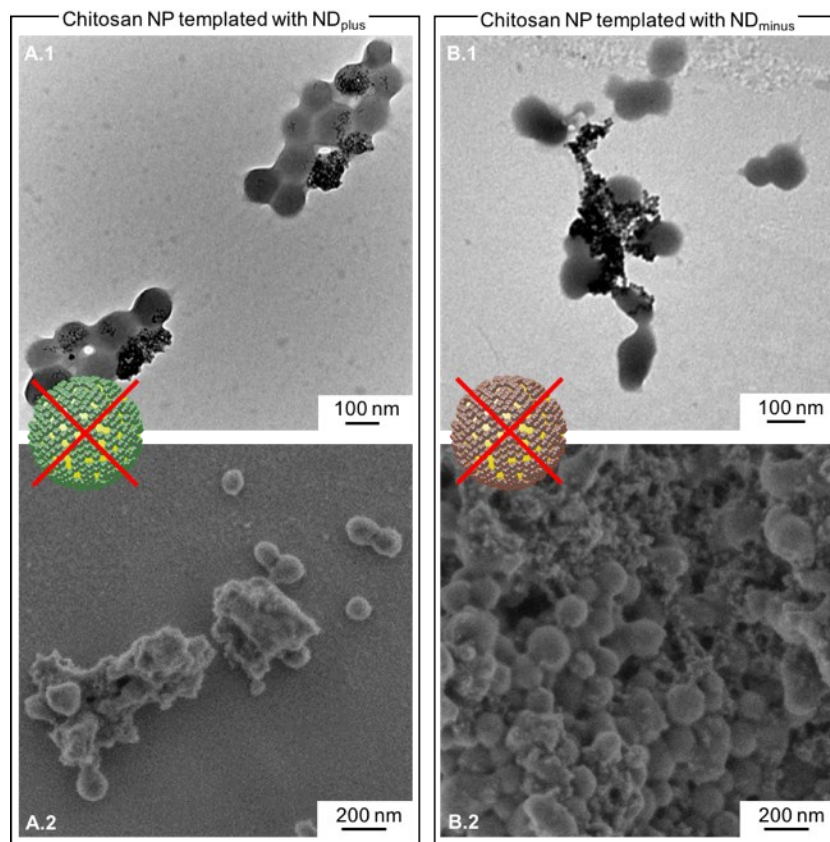


Fig. S 4: TEM and SEM micrographs for unsuccessful attempts to template chitosan particles with nanodiamonds. We mainly observed the formation of aggregates as depicted in micrographs. This can most likely be attributed to the intrinsic tendency of the nanodiamonds to aggregate also without the presence of any chitosan molecules or particles.

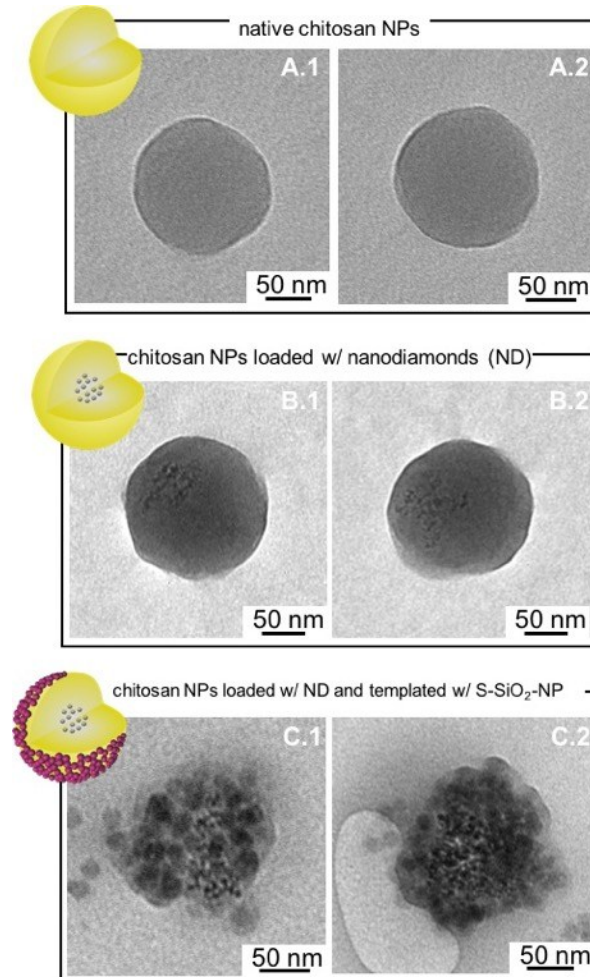


Fig. S 5: TEM micrographs of A) native chitosan NP, B) ND loaded chitosan NP, and C) ND loaded and S-SiO₂-NP templated chitosan NP further visualizing the the loading and templating capacities of the chitosan NP

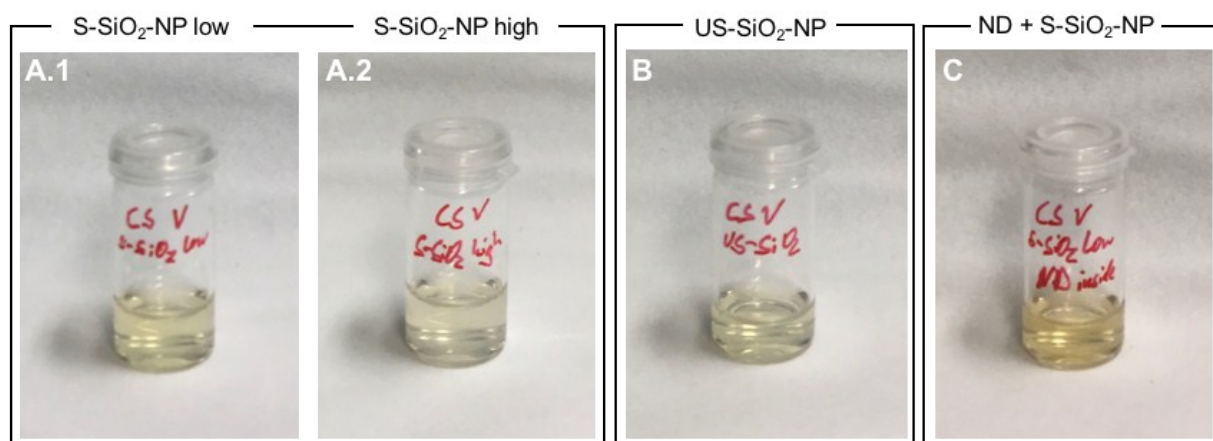


Fig. S 6: Photographs of dialyzed chitosan supraparticle dispersions. The dispersions showed no sedimentation at any point after the dialysis process.